# iScience

**Article**

# Real-time and automated monitoring of antischistosomal drug activity profiles for screening of compound libraries



Drug library

8-microwell chip

x16

Real-time and parallelized impedance-based detection

~20 parasite larvae per microwell

Larval movement

*Alive*

*Dead*

Time    x128

Paolo S. Ravaynia, Stefan Biendl, Francesco Grassi, Jennifer Keiser, Andreas Hierlemann, Mario M. Modena

paolo.ravaynia@bsse.ethz.ch

**Highlights**

Scalable, plastic microwell chip with integrated platinum electrodes

Automated impedance-based recording of 128 microwell units in parallel

Continuous monitoring of *in vitro* drug library efficacy on schistosomula for 72 h

Identification of four fast-acting antischistosomal drugs for *in vivo* testing
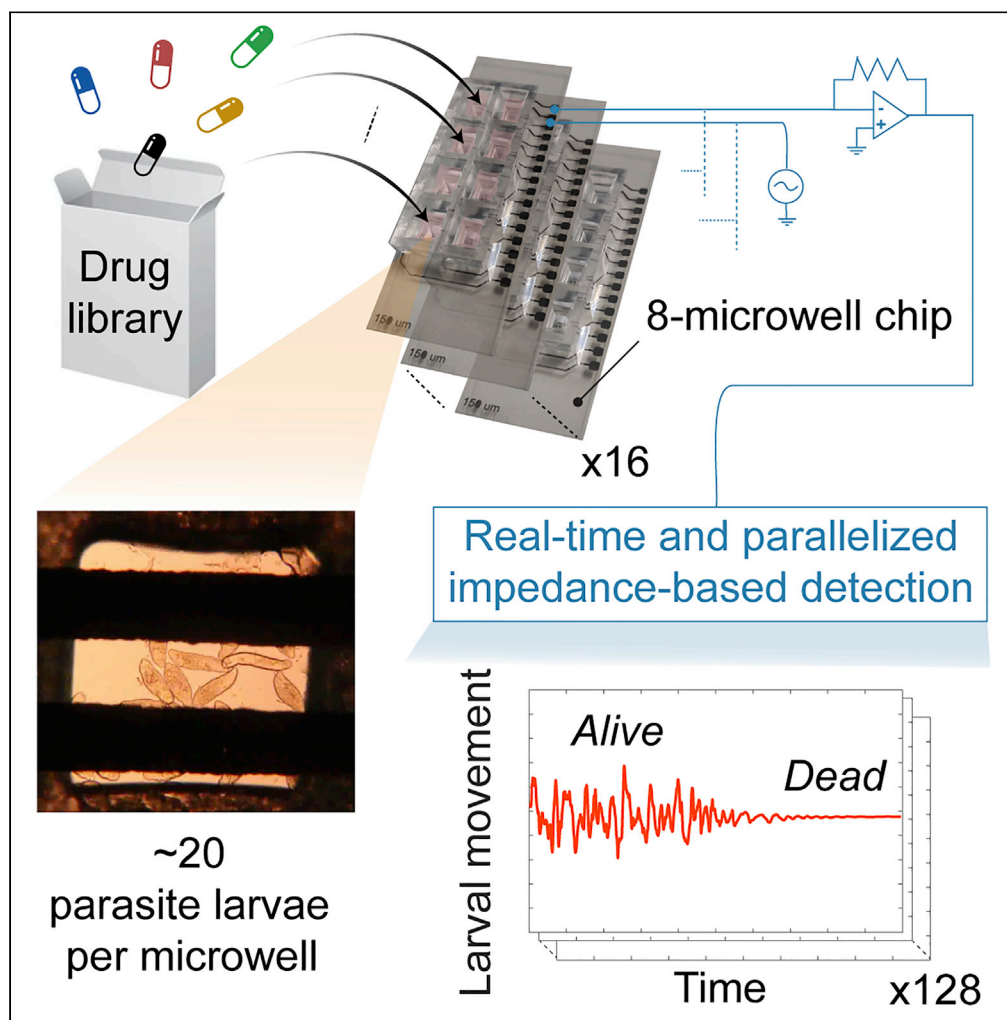
Article

# Real-time and automated monitoring of antischistosomal drug activity profiles for screening of compound libraries

Paolo S. Ravaynia,[1,4,*] Stefan Biendl,[2] Francesco Grassi,[3] Jennifer Keiser,[2] Andreas Hierlemann,[1] and Mario M. Modena[1]

## SUMMARY

**Schistosomiasis is a neglected tropical disease that affects over 200 million people annually. As the antischistosomal drug pipeline is currently empty, repurposing of compound libraries has become a source for accelerating drug development, which demands the implementation of high-throughput and efficient screening strategies. Here, we present a parallelized impedance-based platform for continuous and automated viability evaluation of *Schistosoma mansoni* schistosomula in 128 microwells during 72 h to identify antischistosomal hits *in vitro*. By initially screening 57 repurposed compounds against larvae, five drugs are identified, which reduce parasite viability by more than 70%. The activity profiles of the selected drugs are then investigated via real-time dose-response monitoring, and four compounds reveal high potency and rapid action, which renders them suitable candidates for follow-up tests against adult parasites. The study shows that our device is a reliable tool for real-time drug screening analysis of libraries to identify new promising therapeutics against schistosomiasis.**

## INTRODUCTION

Schistosomiasis affects annually more than 200 million people worldwide (Vos et al., 2017; McManus et al., 2018). Among human parasitic diseases, schistosomiasis ranks third after malaria and intestinal nematode infections in terms of socioeconomic and public health burden, especially in tropical areas (Adenowo et al., 2015; Olveda et al., 2016; Kyu et al., 2018). The infection occurs through exposure to a parasitic trematode of the genus *Schistosoma*, which penetrates human skin during contact with contaminated water and damages urogenital, intestinal, and hepatic functions by depositing eggs in the blood vessels surrounding the bladder, intestines, and/or liver (Gryseels, 2012). Currently, no vaccine is available to prevent infection, and treatment relies exclusively on a single drug, praziquantel (PZQ), developed in the 1980s (Vale et al., 2017; Molehin, 2020). Despite the high efficacy and low cost of PZQ, there is a risk of developing resistance, as the drug has been widely adopted for morbidity control in endemic areas for more than four decades (Wang et al., 2012; Bergquist et al., 2017). In addition, the current drug-discovery pipeline for schistosomiasis is alarmingly unproductive because of the low commercial investments for neglected tropical diseases and limited-throughput of standard phenotypic visual screening (Conteh et al., 2010; Weng et al., 2018). Thus, reliable and easy-to-use high-throughput screening systems are urgently needed to speed up the antischistosomal drug development process and to identify new lead compounds against the human parasite *Schistosoma mansoni*.

The microscopic assessment of schistosome viability by a trained operator is considered the gold standard of assessing drug efficacy, as it can be easily applied to all parasite stages in *in vitro* and *ex vivo* drug studies. However, this laborious and time-consuming procedure has limited throughput, is affected by a high degree of subjectivity of the examiner, and delays the discovery of new compounds (Ramirez et al., 2007; Lombardo et al., 2019). The possibility of using either larval-stage worms or newly transformed schistosomula (NTS), which are artificially obtained in large numbers by the successful establishment of the life cycle of *S. mansoni* in the laboratory, has opened routes for developing high-throughput approaches for antischistosomal drug screening (Abdulla et al., 2009; Keiser, 2010; Peak and Hoffmann, 2011). Dye-based and colorimetric-based high-throughput assays have been developed for automated detection of larvae viability; however, the required number of parasites per well was very large in comparison to the standard

[1]Bioengineering Laboratory, Department of Biosystems Science and Engineering, ETH Zürich, Mattenstrasse 26, 4058 Basel, Switzerland

[2]Swiss Tropical and Public Health Institute, Department of Medical Parasitology and Infection Biology, University of Basel, Socinstrasse 57, 4051 Basel, Switzerland

[3]Centre for Microsystems Technology, Department of Electronics and Information Systems, Ghent University, Technologiepark-Zwijnaarde 126, 9052 Gent, Belgium

[4]Lead contact

*Correspondence:
paolo.ravaynia@bsse.ethz.ch
https://doi.org/10.1016/j.isci.2022.104087

visual method for drug testing (Peak et al., 2010; Panic et al., 2015b; Aguiar et al., 2017). As an alternative, image-based automated microscopy systems have been implemented to assess and quantify larval motility and morphology during drug screening (Paveley et al., 2012; Chen et al., 2020). In addition, the development of highly efficient image-analysis protocols has enabled the automatic identification of parasite larvae and the tracking of their movement and phenotype changes via video acquisition using conventional microscope and computer resources (Singh et al., 2009; Lee et al., 2012; Marcellino et al., 2012; Asarnow and Singh, 2013). However, continuous evaluation of NTS viability via imaging-based tools for large-scale drug-exposure assays often requires specialized equipment, such as lab-automation robotic equipment and automated, high-content screening microscopes for rapid analysis of multiple plates, which may ultimately limit its widespread use in common laboratory settings. Finally, a simple, label-free, high-throughput impedance-based technique has been successfully applied on cercariae and adults for monitoring and quantifying their motility; nonetheless, this system could not be used to detect schistosomula movements (Rinaldi et al., 2015). Hence, there is a demand for advanced platforms that are capable of large-scale assessment of NTS viability in an automated and continuous way.

Besides the development of novel screening technologies, new antischistosomal therapeutics are direly needed, as the drug development pipeline is dry and not sufficiently supported by pharmaceutical companies (Trouiller et al., 2002; Pedrique et al., 2013). For neglected tropical diseases, repurposing (or repositioning) of drugs, which have been already tested for other indications in humans, is an essential strategy. This approach can help to accelerate the discovery of anthelmintic treatments, thereby saving costs and time in the drug development process by facilitating transition from preclinical studies to clinical trials (Panic et al., 2014, 2015a). Therefore, libraries of compounds for repurposing of nonprofit organizations, such as the *Drugs for Neglected Diseases Initiative* (DNDi) and *Medicines for Malaria Venture* (MMV), offer an important resource for identifying novel lead drugs. To make optimal use of these libraries, simple and automated high-throughput tools are strongly required to implement an efficient and cost-effective screening.

In a previous study, we demonstrated that microstructured well plates help to reduce compound volumes and the number of parasites needed for testing and allow for schistosomula culturing. Moreover, the use of microstructures well plates enables the detection of NTS motility, which has been established as a reliable descriptor of schistosomula viability, by means of electrical impedance spectroscopy (EIS) (Modena et al., 2017; Chawla et al., 2018; Lombardo et al., 2019; Ravaynia et al., 2020). EIS is a noninvasive and label-free technique for investigating the dielectric-property variations of a target sample over a specific range of frequencies in real time (Sun and Morgan, 2010). The previously developed small-scale EIS platform included only 32 microwell units and was validated for continuous assessments of dose-response effects of four established drugs on NTS viability by comparison with standard visual scoring (Ravaynia et al., 2020). However, the adopted rapid-prototyping material, polydimethylsiloxane (PDMS), is known for small-molecule absorption, which often obviates the use of microfluidic analytical platforms that have been developed in academic labs for drug-screening applications and is not amenable to large-scale fabrication. Therefore, the implementation of a higher-throughput impedance-based device with reliable drug-activity assessment has to be addressed to boost the antischistosomal screening in both academic and highly standardized industrial settings.

Here, we present the development and use of a fully integrated and automated impedance-based system, featuring a large number of parasite compartments (128), for parallel drug screening of potential antischistosomal compounds with minimal operator intervention. For reliable application in drug discovery, we adopted a standard laboratory plastic material, polystyrene, (PS) to avoid compound adsorption and absorption, to reduce fabrication costs and time, and to increase measurement throughput (Van Midwoud et al., 2012; van Meer et al., 2017). The developed device offers simultaneous measurements in 128 microwells in parallel, which corresponds to more than 30 drug exposure scenarios with four statistical replicates in a single assay. Moreover, we were able to implement a setup to run automated multiday assays with continuous detection of parasite viability that drastically reduced experimental efforts. The system included four modular platforms in standard microtiter-plate formats, which ensured full compatibility with lab automation tools. In an exemplary drug screening study, we analyzed the activity of 57 compounds, which were selected in an end-point phenotypic drug sensitivity assay from the MMV Pandemic Response Box (PRB) (Biendl et al., 2021), over 3 days by means of continuous impedance monitoring. We then identified the five most active antischistosomal drugs and assessed temporal characteristics of dose-dependent

responses of the NTS. The obtained results prove that our highly-parallelized modular plastic platform represents a powerful tool for continuous long-term measurements of the activity of compound libraries on schistosomula, thereby significantly advancing drug-screening for schistosomiasis.

## RESULTS

### Highly parallelized platform for antischistosomal drug screening

We developed an integrated microwell plastic chip to establish reliable and automated impedance-based monitoring of schistosomula motility after exposure to compounds from large drug libraries (Figure 1A). The chip was fabricated using polystyrene (PS), a standard and well-characterized laboratory plastic material, to avoid absorption and/or adsorption of small hydrophobic drug molecules (van Meer et al., 2017; Ravaynia et al., 2020). The PS chips were produced using injection molding, which allowed for high-volume and low-cost fabrication (Figure S1). Each chip included a top PS layer ($13 \times 38$ mm$^2$) featuring eight microwell units, which were sealed via double-sided adhesive tape to a polyethylene terephthalate (PET) foil ($20 \times 61.5$ mm$^2$), equipped with eight pairs of coplanar platinum electrodes for electrical monitoring of parasite movements. The top-open reservoir microwells were arranged at a 9-mm pitch to allow for loading of the parasite larvae and compound solutions with standard multichannel pipettes, which facilitated system operation. The small microwell volume and dimensions (65 μL, 5 mm in height) resulted in fast and reliable sedimentation of the NTS onto the electrodes (within ∼3 min, Figure 1B). Moreover, the geometry and physical dimensions of the electrodes and microwells were optimized to achieve high sensitivity in the volume extending to a 100-μm height above the electrodes, which is in the same range as the size of the NTS ($\sim 50 \times 100$ μm$^2$), as previously described (Ravaynia et al., 2020). To provide enough throughput for drug screening applications, the platform could accommodate 4 PS chips, and up to four platforms could be stacked in an incubator to simultaneously record from 16 chips, so that 128 conditions could be assessed in a single run (Figure 1C). Each platform included a printed circuit board for signal multiplexing and an aluminum holder frame to place the chips. In addition, a PS lid was inserted into each chip-holder frame to cover the open microwell structures and limit evaporation during multiday assays (Figure S2A) so as to minimize operator interference.

The developed highly parallelized impedance-based (HPI) system enabled parallel operation of multiple 8-microwell plastic chips and featured a high level of modularity to ensure flexibility and straightforward assembly and sample loading. An electrical-equivalent circuit model of a well with the integrated electrodes, selected among four platforms, is illustrated in Figure 1D. A microwell unit can be modeled as a variable impedance $Z_w$, which represents the NTS suspension between the electrodes, in series with the resistance of the metal traces on the PET foil and a double-layer capacitance $C_{dl}$, which is formed at the interface between the platinum electrodes and the medium. To estimate parasite motility, we applied a 500-kHz potential (100 mV) to the selected electrode pair and measured the relative fluctuations of $Z_w$ over time, which were caused by the movement of the parasites in between the electrodes, while the average absolute value of the impedance only contained information on solution resistivity and parasite number (Figure S3). The multiplexing of the 128 units was performed by an intermediate controller motherboard, which interfaced the lock-in amplifier and the multiplexers and demultiplexers (mux/demux) of each platform for transferring the AC signal to the selected measurement units. Each microwell of the four platforms was sampled at 32 Hz during a 1-min window to detect signal fluctuations caused by the NTS movements and was measured every 16 min during the experiments to achieve quasi-continuous analysis of drug-induced motility variations.

The preparation and execution of the impedance-based drug assay with the HPI system were performed on two consecutive days to ensure easy and robust parasite handling (Figure 2). On day −1, the chips were loaded with 30 μL of culture medium for pre-wetting the microwells using a multichannel pipette. The overnight incubation of the chips with plain medium solution, preceded by a 10-min solution degassing, was implemented to remove small air bubbles that could form at the bottom of the microwell compartments and could interfere with the sedimentation and detection of the parasites. On day 0, we first removed the pre-wetting medium and then loaded 30-μL larvae solution with ∼0.7 NTS μL$^{-1}$ so that 20–25 NTS were loaded into each well. This procedure ensured simple and bubble-free NTS dispensing to all 128 units. We then performed impedance measurements of all the microwells for 1 h to evaluate the initial signal fluctuations of untreated parasites and to confirm correct sample loading. This operation also helped to establish a motility index value for each unit to be able to monitor how the motility of the parasites changed during the assay and to compare measurements of microwells with different numbers
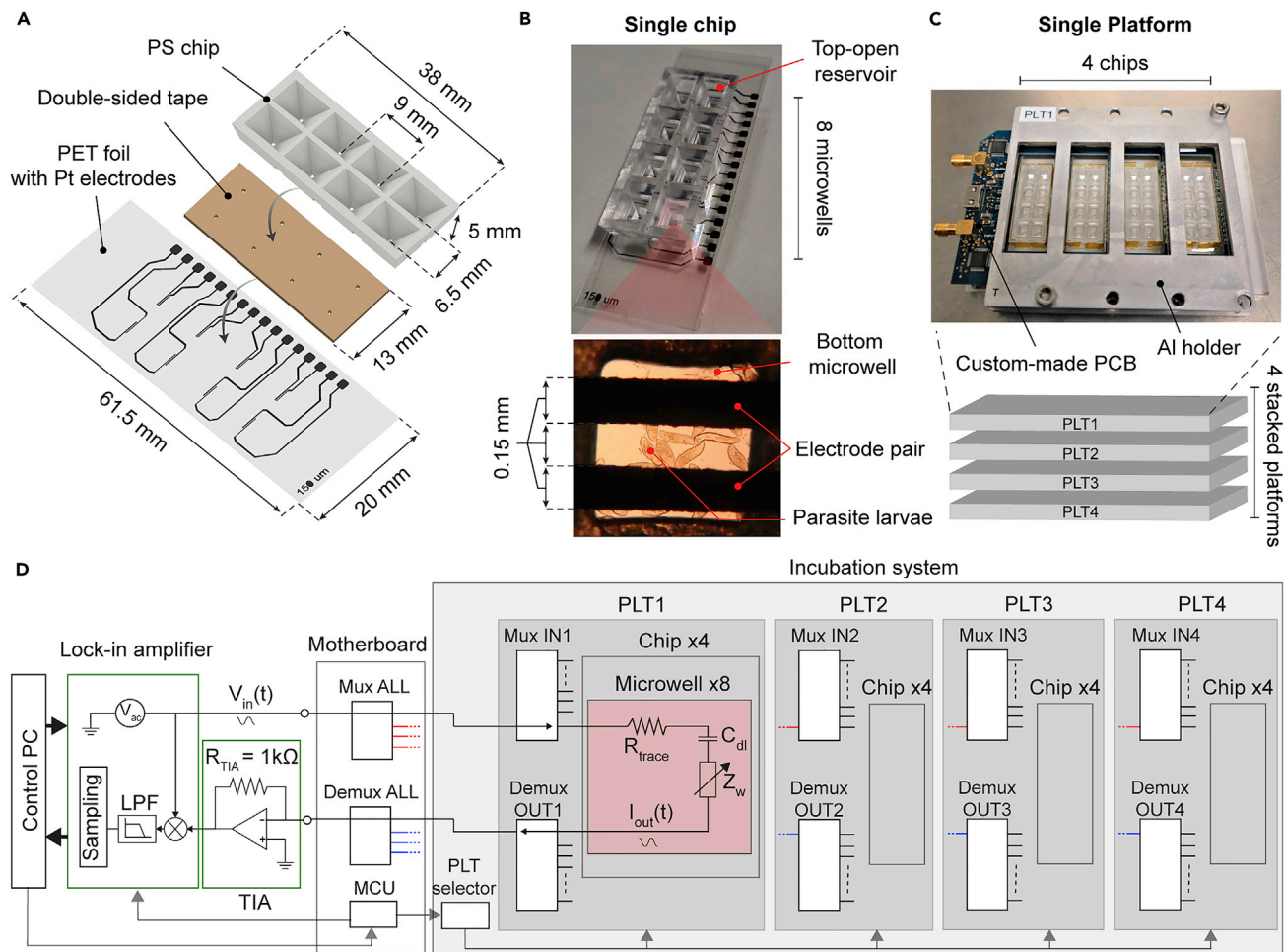
**Figure 1. Layout of the modular plastic highly parallelized impedance-based (HPI) system**

(A) The chips were fabricated using two transparent plastic components: an injection-molded polystyrene (PS) microwell layer and a polyethylene terephthalate (PET) slide patterned with platinum (Pt) electrodes. The two parts were then sealed together with a double-sided adhesive tape featuring eight laser-cut holes, which provided access to the electrode pairs for impedance detection.

(B) A single plastic chip featured eight individual testing microwells with top-open reservoir cavities, shaped as an inverted pyramid to promote sedimentation of the parasites to the sensing volume above the coplanar electrodes.

(C) Each platform (PLT) could accommodate up to four chips, which were placed in between a custom-made printed circuit board (PCB) and an aluminum (Al) holder. Up to four platforms could be measured in parallel for a single experiment.

(D) The electrical equivalent circuit of the modular impedance-based system included a lock-in amplifier for generating the AC voltage signal ($V_{in}$), a motherboard for routing the signal to the selected unit of an 8-microwell chip, and a *trans*-impedance amplifier (TIA) for current-to-voltage conversion. The voltage signal was finally routed to the input of the lock-in amplifier, where it was multiplied with $V_{in}$, low-pass filtered (LPF) and sampled, and subsequently stored on a control PC. A microcontroller unit (MCU) soldered on the motherboard was used for routing and multiplexing of the four individual platforms and for synchronizing the switching between the 128 microwells and the lock-in amplifier (see also Figures S1–S3 and S10).

of parasites (for normalization details, see also Figure S4) (Chawla et al., 2018). After the acquisition of larval baseline activity, 30 μL of drug solution were added to the units, each condition in quadruplicates, and the motility of the NTS exposed to the compounds was recorded continuously for 3 days in the four platforms without any intervention by the operator. The controls were also included in each assay in quadruplicates, and the NTS for controls were cultured in a standard medium and a medium containing the drug vehicle (0.5% DMSO). Therefore, a single assay could accommodate up to 30 different compound exposures and two controls in quadruplicates. At the end of each drug assay, we confirmed that the long-term impedance-based measurements showed Z′-factor scores above 0.5 and signal-windows higher than 2, as recommended by the NIH guidelines for drug screening (Table S1) (Sittampalam et al., 2004; Macarró and Hertzberg, 2011).
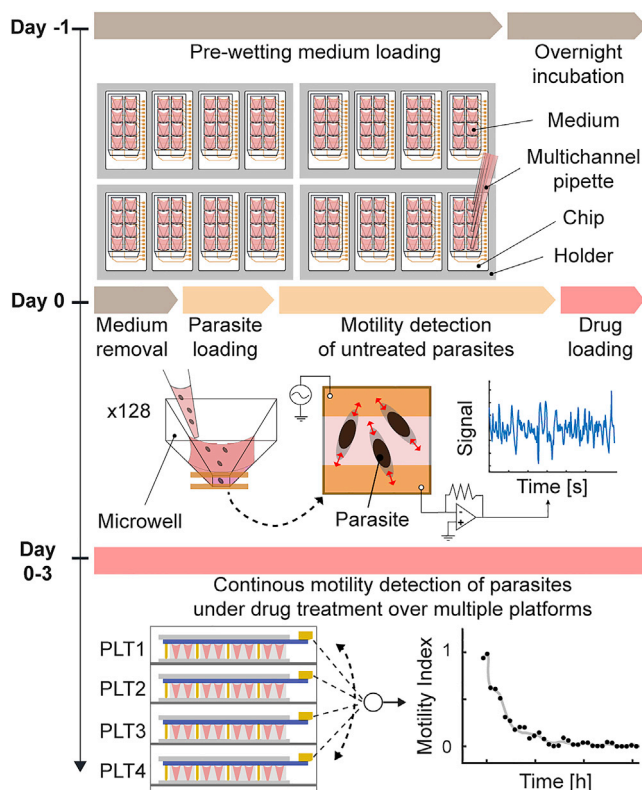
**Figure 2. Operation of the automated highly parallelized impedance-based (HPI) device**

The experimental timeline is shown at the left side, whereas the corresponding steps for performing the impedance-based assay are displayed at the right. On day −1, all 16 chips were first loaded with 30 μL of standard medium using a multichannel pipette. On day 0, after an overnight degassing of the plain medium in the chips, 25 μL of culture medium in each microwell were replaced by 30 μL of NTS solution. Impedance-based motility detection of untreated parasites was then performed for 1 h before adding 30 μL of drug solution into each PS microwell. During the 3 days of drug exposure, the impedance detection of schistosomula status was continuously running without operator interference and by switching every 4 min between the four stacked platforms (PLT). The drug-induced NTS motility variations from all 128 wells were continuously recorded until the end of the assay (see also Figure S4 and Table S1).

## Sensitivity assays for antischistosomal drug discovery

The overall screening workflow executed through standard visual inspection and automated impedance-based detection is presented in Figure 3A. For a first assessment of the antischistosomal activity of the PRB drugs with an established end-point and time-limited assay, the library (400 compounds) was initially screened against *S. mansoni* larvae using operator-based visual phenotypic evaluation. In this preliminary screening, ∼100 NTS in 200 μL solution were loaded into each well of a 96-well plate, and were subsequently exposed to a 10 μM concentration of the PRB drugs (Figure 3B). After 72 h of compound incubation, the phenotypic parasite behavior was visually evaluated for each condition according to the standard scoring method (Lombardo et al., 2019; Biendl et al., 2021). To deeply investigate the heterogeneity in dynamic drug responses of NTS that would be missed by standard end-point evaluations in our analysis, we selected a sub-library of 57 compounds from the PRB, which included all highly active drugs and additional inactive compounds. With this approach, we included a large range of *in vitro* compound activity, from 0 to 100% (completely inactive to very active compounds against NTS) in our investigation. The selection also matched the composition of the entire MMV drug collection including similar fractions of antibacterial, antiviral, or antifungal compounds (see Figure S5).

The 57 selected drugs were subsequently analyzed with our HPI device to characterize in a continuous and automated manner, based on their broad spectrum of activity profiles on NTS (Figure 3A). The impedance screening was implemented by dispensing ∼25 NTS in 65 μL of medium containing a 10-μM concentration of the PRB compounds into each unit of the 8-microwell chip (Figure 3C). By continuously recording the
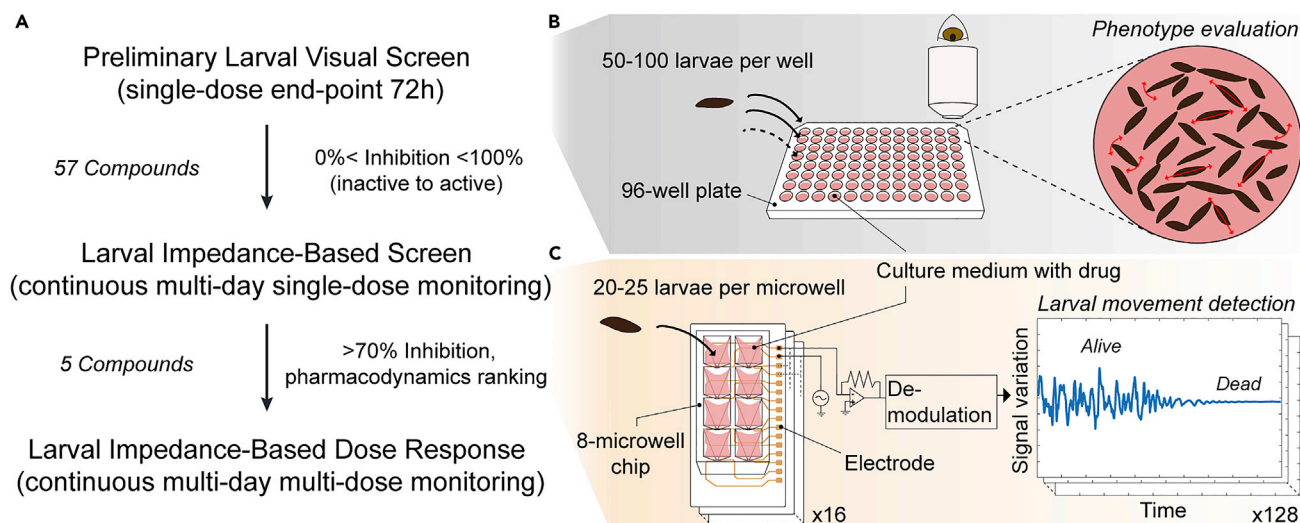
**Figure 3. Visual and impedance-based evaluation for *in vitro* screening of the Pandemic Response Box (PRB) library against *S. mansoni* larvae**

(A) The screening sequence started by scoring the activity of the entire PRB on NTS using standard visual inspection after 72 h of drug incubation. Then, 57 compounds were selected, which represented the entire range of visually observed activity effects, and analyzed by using the automated impedance-based system (see also Figure S5). After 3 days of continuous impedance-based monitoring of drug efficacy, the five most active antischistosomal compounds were identified and ranked. The key criterion included a reduction of NTS viability index by more than 70%. Finally, the selected hits were further characterized by continuous dose-response analysis on the chip.

(B) The visual phenotypic screen was carried out by loading 50–100 NTS in each well of a 96-well plate, which contained culture medium and test compounds at 10 μM (single dose). After 3 days of drug exposure, the operator scored the morphology and the motility of the NTS in each well under the microscope.

(C) For the automated impedance-based screening, each well of an 8-microwell chip was loaded with 20–25 parasites in culture medium with 10 μM (single dose) of the test compound. Every microwell was equipped with a pair of coplanar electrodes for detecting NTS motility by measuring AC impedance variations between the electrodes. By recording the signal fluctuations caused by larvae movements in each well of the 16 chips, which were used in parallel (total of 128 wells), the real-time pharmacodynamic activity of each drug was acquired during 72 h.

drug-induced NTS motility variations as proxy for viability in all 128 microwells in parallel, we assessed the *in vitro* activity profile of each compound to identify the best-performing antischistosomal drugs, which showed an activity inhibition of more than 70% after 3 days of exposure. Although variations in NTS morphology caused by the drug treatment may have an effect on the impedance signal, the power of the signal fluctuations is mainly proportional to NTS motility and is therefore largely unaffected by morphological changes (Chawla et al., 2018). To further investigate the temporal evolution and dose-dependent characteristics of the most active drugs, we finally analyzed the potency of the hits compounds in a dose-response assay with six different concentrations (1.5, 3, 6, 12, 25, and 50 μM) during 72 h of continuous measurement by using our automated device again.

## Multi-day monitoring of the Pandemic Response Box subset efficacy

The impedance-based results of the continuous 3-day motility monitoring of NTS, incubated with the 57 selected drugs at 10 μM, are shown in Figure 4A. The HPI system allowed for differentiating inhibitory (motility$_{drug}$ < motility$_{control}$) and excitatory (motility$_{drug}$ > motility$_{control}$) compound effects — both transient and permanent — on the parasite larvae behaviors (for the characterization of reference antischistosomal drugs see also Figure S6). Seven drugs (A-G6, A-H2, C-C5, E-A6, E-B8, E-D5, and E-G4) caused a substantial fast transient or permanent decrease in motility (>40%) during the first 10 h of continuous measurements in comparison to vehicle control conditions. In contrast, four compounds (C-F5, D-A3, D-A4, and E-B3) caused a significant transient or sustained increase (>30%) in NTS motility during the first 20 h of evaluation. Moreover, we compared the rapid transient maximum inhibition of the two most effective compounds, C-C5 and A-H2, to the minimum motility value of the vehicle control condition within the same time window (first 5 h) using the Kruskal-Wallis test, followed by Dunn-Sidák test (Figure S7A). In this comparison, the motility indices of the replicates treated with 10 μM A-H2 were significantly smaller (0.27 ± 0.09, p < 0.01) than that of the controls in DMSO (0.81 ± 0.06). The same analysis was performed for the fast-acting compounds causing strong excitation: D-A3 and E-B3. We found a significant difference (p < 0.01) between the motility indices of parasites treated with 10 μM of E-B3 (1.63 ± 0.17) and those of the vehicle control (1.09 ± 0.05) during the first 10 h (Figure S7B).
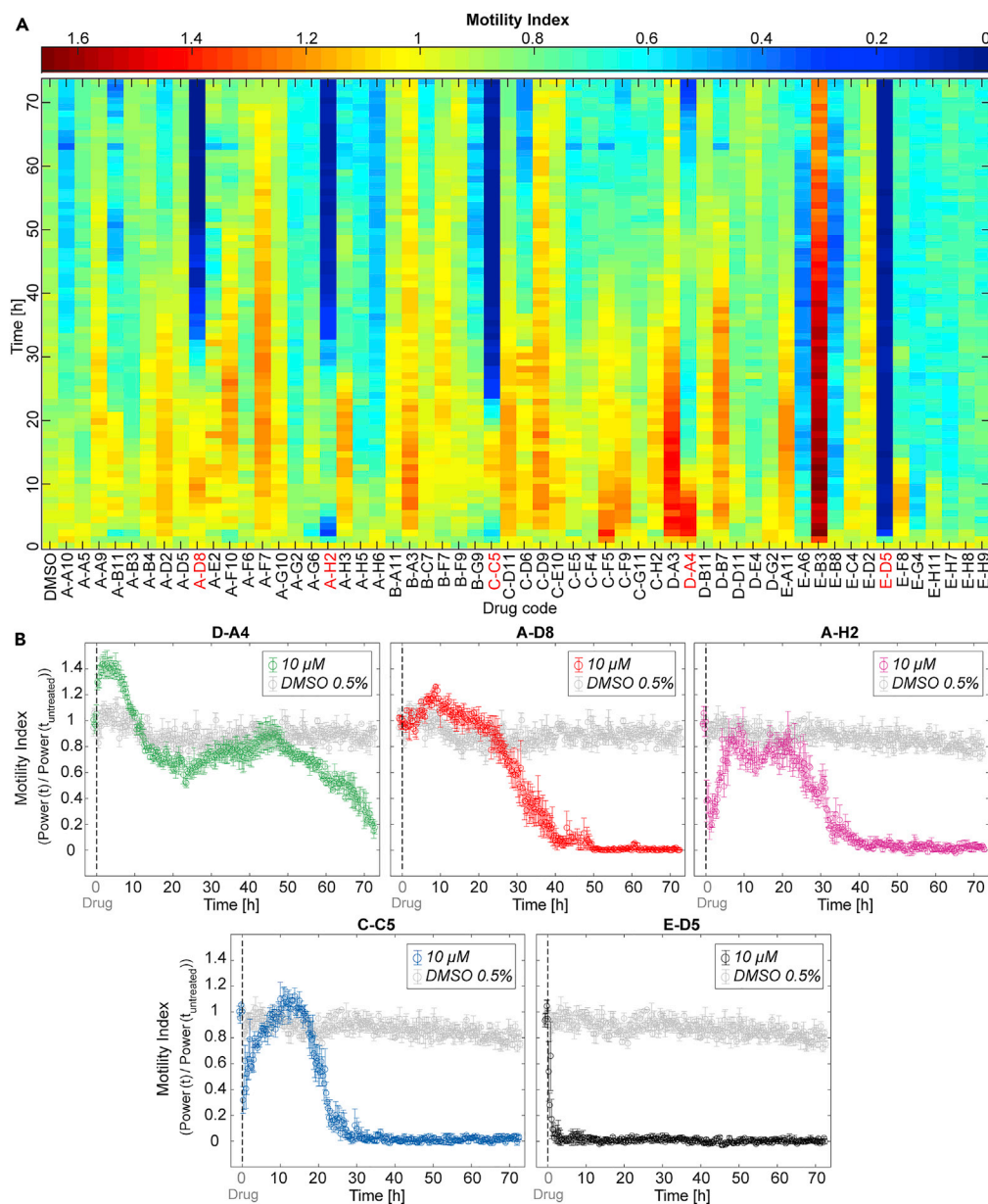
**Figure 4. Monitoring of larval motility during *in vitro* testing of the selected Pandemic Response Box (PRB) drugs through impedance-based continuous measurements**

(A) The heat map shows the variations in the motility index of NTS upon exposure to the 57 test compounds during 72 h of real-time acquisition with the HPI device. Colors of the top scale bar indicate the NTS motility levels upon exposure to the drugs, which were normalized to the 1-h pretreatment phase. All PRB drugs were applied at 10 μM in quadruplicates, and each color box represents the average parasite motility response (average of four wells) to each compound every hour. The codes of the five best-performing drugs are highlighted in red.

(B) The motility graphs show the NTS responses to the five hit compounds, identified during the screening, which were compared to the vehicle-control sample (parasites in 0.5% v/v DMSO, in gray color). The vertical dashed lines indicate the times at which the drugs were dosed. Each circle represents the mean value of the motility index, measured in parallel and averaged over four microwells every 16 min. Error bars indicate the SE of the mean (see also Figures S6–S8 and Table S2).

By applying a threshold of 70% relative inhibition of parasite viability (motility index upon drug exposure normalized to that of vehicle controls) (Ravaynia et al., 2020) after 72 h of constant drug exposure, five hit compounds (E-D5/MMV688991, C-C5/MMV1578555, A-H2/MMV1634491, A-D8/MMV1582497, and D-A4/MMV394033) were selected for further evaluation and ranked according to their dynamics using
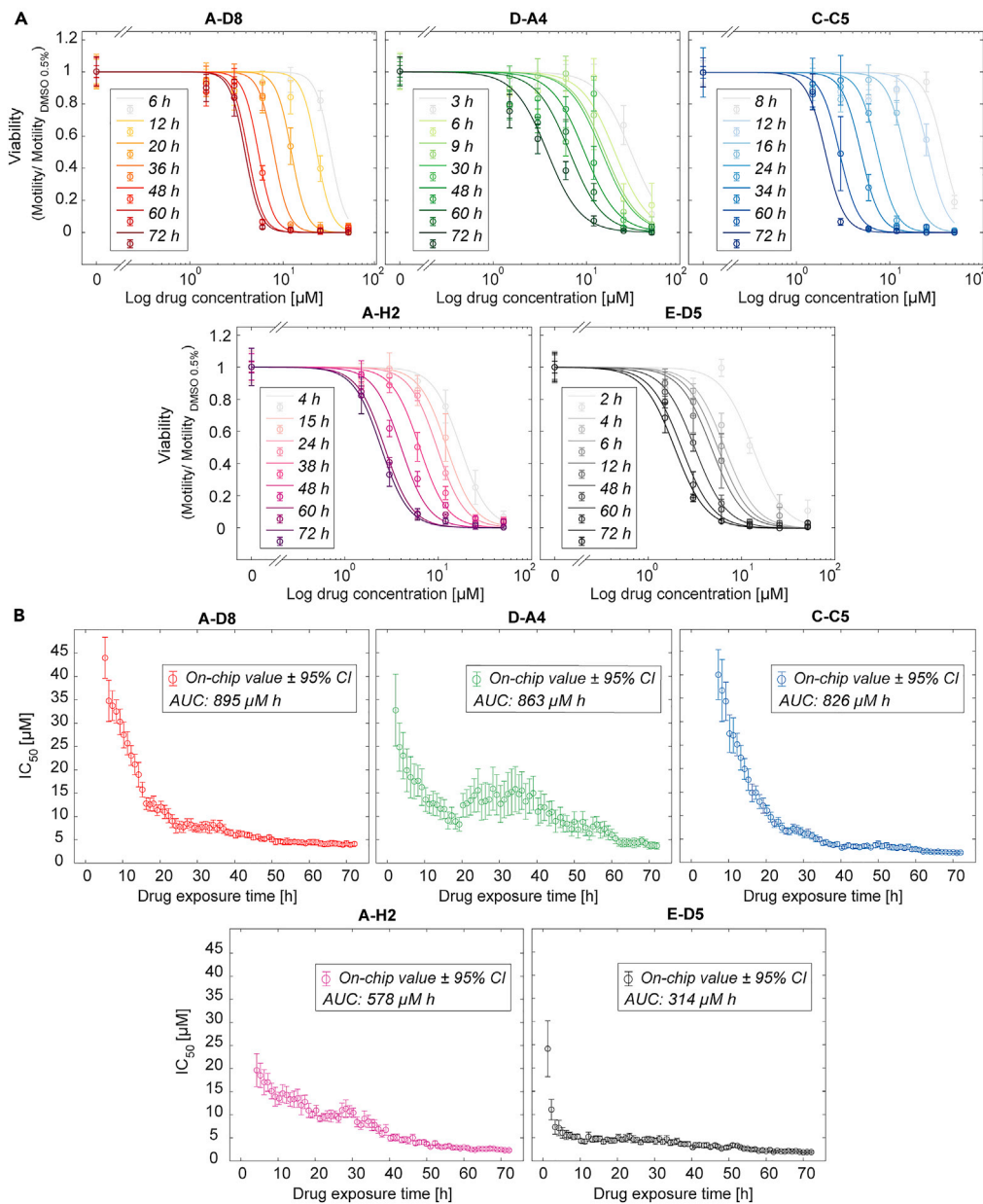
**Figure 5. Continuous dose-response characterization of the five hit compounds by long-term impedance-based assessment of NTS viability**

(A) The graphs show the impedance-based estimations of schistosomula viability at seven selected time points as a function of the drug concentration for all hits. The NTS were incubated with six different concentrations (1.5, 3, 6, 12, 25, and 50 μM) of each compound and monitored during 72 h. Each circle represents the mean viability value of four replicates, normalized to the vehicle control condition (NTS in 0.5% v/v DMSO). Error bars indicate the SE of the mean. The sigmoidal fits were used to calculate the $IC_{50}$ value at each time point for the five drugs.

(B) The plots display the temporal evolution of the $IC_{50}$ values for the five selected compounds. The $IC_{50}$ estimations were calculated from the impedance-based measurement data of NTS viability. Error bars show the 95% CIs. In the figure legends, the area-under-the-curve (AUC) values are also reported (see also Figure S9, Tables S3 and S4).

the impedance-based screen (Figure 4B; for viability and phenotypic details see also Figure S8 and Table S2 and). E-D5 exhibited the fastest *in vitro* lethal effect on schistosomula, which occurred 3 h after drug dosage. The second fast-killing compound was C-C5, which led to complete inhibition of parasite motility at 25–30 h. We selected two more drugs (A-H2 and A-D8), which displayed a similar response

and a high killing efficacy after around 40 h of incubation. Finally, a last compound was selected (D-A4), which showed a peculiar biphasic NTS response profile over 3 days of measurements, with a transient excitation in the first 10 h, followed by a delayed monotonic motility decrease during the last 30 h of continuous monitoring, reaching a final motility index value of ∼0.2.

### Continuous dose-response characterization of the five hit compounds

We then added six serially-diluted concentrations (1.5, 3, 6, 12, 25, and 50 μM) of A-D8, D-A4, C-C5, A-H2, and E-D5 to the HPI system to characterize, in real time, the dose-dependent responses of the NTS during 72 h. The long-term dose-response curves of the five hit compounds are shown in Figure 5A (the real-time motility indexes are reported in Figure S9). The viability of the larvae exposed to the highest drug concentrations (50 and 25 μM) of A-D8 dropped to zero within the first 20 h, indicating that the NTS were killed by the compound at these doses. In the case of NTS exposure to 12 and 6 μM of A-D8, parasite viability ceased after 36 and 60 h, respectively. For the two lower concentrations (3 and 1.5 μM), the larvae remained viable and displayed good motility levels during the entire assay. 50 and 25 μM dosages of D-A4 showed high activity after 9 and 30 h, whereas 12 μM caused full inhibition at 72 h, displaying again the biphasic NTS response that had been observed for 10 μM in the screening phase (Figures 4B and S9). For lower concentrations (6 and 3 μM) of D-A4, we noticed a considerable reduction in viability ($0.58 \pm 0.09$ and $0.38 \pm 0.06$) after 3 days. The third hit compound (C-C5) exhibited a slight time delay (10–20 h) for killing the parasite at the highest doses due to an initial inhibition-and-recovery pattern that had been observed in the preceding 10-μM test (Figures 4B and S9). Nonetheless, all concentrations larger than 3 μM efficiently caused NTS death within the 72 h exposure. The lethal effect of A-H2 against schistosomula for the two highest concentrations appeared already after 10 h; however, longer exposure times were required for 12 and 6 μM, which showed complete inhibition of parasite viability after 48 and 72 h, respectively. With E-D5, we obtained dose-response curves indicating higher lethality in comparison to the other tested compounds. The larvae exposed to 50, 25, and 12 μM were dead already after 6 h, whereas those exposed to 6 and 3 μM reached viability indices of $0.03 \pm 0.01$ and $0.19 \pm 0.02$ at 72 h.

The antischistosomal potencies of all hit compounds were further examined and ranked by computing the $IC_{50}$ over time, which corresponds to the concentration at which a 50% inhibition of parasite viability occurs, and by assessing the total effective drug exposure (area under the curve or AUC, Figure 5B). The temporal evolution of the $IC_{50}$ of the less potent compound A-D8 (AUC: 895 μM h) featured a 24-h monotonic decrease to $8.0 \pm 1.6$ μM with values of $5.2 \pm 0.4$ μM at 48 h and $3.9 \pm 0.4$ μM at 72 h. For D-A4 (AUC: 863 μM h), the $IC_{50}$ rapidly dropped to $8.3 \pm 1.5$ μM after 20 h; however, the values then slightly increased between 24 and 48 h because of the biphasic NTS response behavior at lower doses (<12 μM). After 72 h, the potency value of D-A4 was $3.8 \pm 0.7$ μM. The $IC_{50}$ progression of C-C5 (AUC: 826 μM h) displayed a significant decrease over the first two days, reaching $7.4 \pm 1.0$ μM and $3.3 \pm 0.3$ μM at 24 and 48 h. The $IC_{50}$ value did not change considerably over the last 24 h of the evaluation and settled at $2.1 \pm 0.2$ μM. In the case of the second-potent compound A-H2 (AUC: 578 μM h), the $IC_{50}$ decreased during the first day of drug exposure to $9.7 \pm 1.3$ μM, reaching a final value of $2.3 \pm 0.3$ μM after two more days of continuous measurements. Finally, E-D5 (AUC: 314 μM h) was the most-potent and fastest-acting drug in the dose-response assay, featuring an $IC_{50}$ of $7.3 \pm 1.6$ μM after 3 h and reaching a final value of $1.9 \pm 0.2$ μM after 72 h.

## DISCUSSION

In this study, we screened 57 repurposable drugs with the aim of finding novel and promising compounds with high potency, fast action, and low potential developing costs against the larval stage of *S. mansoni* using an impedance-based method (Panic et al., 2014). We selected compounds from the MMV Pandemic Response Box, which contains a collection of structurally diverse molecules with affirmed activity against bacteria, viruses, or fungi. For the *in vitro* screening, we implemented a highly parallelized, impedance-based (HPI) system to measure, continuously and in an automated manner, the viability of *S. mansoni* schistosomula during multiday drug-exposure tests with minimal efforts. The HPI system was able to recognize both excitatory and inhibitory effects of tested PRB compounds on NTS during 72 h of drug exposure (Figure 4A). Interestingly, most of the drugs that rapidly induced hypermotility at 10 μM did not show high antischistosomal activity after the complete assay duration. In contrast, transiently or permanently inhibitory compounds were more successful in killing the NTS within the course of the 10-μM exposure. In addition, few drugs displayed a peculiar biphasic response that could not have been identified without continuous monitoring.

Our single-dose impedance-based screening yielded five antischistosomal hit compounds, which included two antibacterials (A-D8/MMV1582497 and C-C5/MMV1578555), two antivirals (D-A4/MMV394033 and E-D5/MMV688991), and one antifungal (A-H2/MMV1634491). Among these compounds, E-D5, i.e., nitazox-anide, had been previously identified as antischistosomal, which confirms the suitability of our system for drug screening (Abdulla et al., 2009; Maccesi et al., 2019).

For further characterization, we examined the selected five drugs with a continuous dose-response screening using our chips. All compounds showed $IC_{50}$ values below 4 µM after 72 h of exposure, which renders them suitable for *in vitro* follow-up tests on adult-stage parasites. Moreover, the differences in the characteristics of dose-dependent and time-dependent responses of the NTS to each drug highlight the importance of continuous monitoring of parasite activity for testing of promising compounds (Figure S9). Using our impedance-based real-time detection, we revealed the fast action and high efficacy of E-D5, which displayed an $IC_{50}$ of less than 5 µM already after 8 h of incubation, compared to the slower activity decrease upon dosage of A-H2, C-C5, D-A4, and A-D8. By assessing the drug efficacy every 16 min, we could rank the potency of the selected compounds based on the area under the curve (AUC) of the complete $IC_{50}$ temporal transition (Figure 5B). With such an analysis, scientists will have the possibility to prioritize drugs to be promoted to additional preclinical studies not only based on final $IC_{50}$ values but also considering fast action and low effective dose. For example, both compounds, A-H2 and C-C5, featured similar $IC_{50}$ values as E-D5 at 72 h; however, their slower kinetics resulted in a much higher AUC during the whole assay. In addition, although a lower sampling frequency, e.g. every 2 h, might be sufficient to identify fast-acting *in vitro* compounds, the acquisition of multiple data points per hour increases the robustness of the detection and enables to record rapid transitory motility variations that could otherwise be missed.

Recording the temporal evolution of dose-response relationships is also beneficial for comparing drug potency results to other *in vitro* tests that are used for preclinical selection of active compounds. Four of the selected hits (E-D5, A-H2, C-C5, and A-D8) were reported to feature cytotoxicity ($CC_{50}$) values above 20 µM at 48 h (cytotoxicity is commonly measured with Chinese hamster ovarian (CHO) cells), which yields an average $CC_{50}/IC_{50}$ ratio of more than four for these compounds (Table S3) (Reader et al., 2021). Conversely, the $CC_{50}$ value of D-A4 was reported to be 1.4 µM, resulting in a comparably low $CC_{50}/IC_{50}$ ratio (Reader et al., 2021). Therefore, the remaining four drugs should be prioritized for testing against adult schistosomes owing to their sufficiently high *in vitro* efficacy/cytotoxicity ratio. Furthermore, all these four compounds feature favorable physicochemical properties indicated by the compliance with the Lipinski's rules-of-five, a rule of thumb to determine if a chemical compound is likely orally active drug in humans, as oral administration would be the preferred mode for schistosomiasis treatment (Table S4) (Ferrari et al., 2003; Lipinski et al., 2012). Fast action, low cytotoxicity and compliance with Lipinski's rule render these compounds potentially attractive for antischistosomal drug development.

The developed HPI system addresses some major limitations of the standard visual-screening approach, namely the relatively large number of required parasites (50–100) per well for observation, the need of highly-trained staff for the evaluation of parasite viability, and the labor-intensive phenotypic evaluation, all of which ultimately limit the number of analyses per assay. The HPI system enables to continuously measure NTS viability during multiday drug screening and to record dose-response curves with minimal operator intervention. By making use of miniaturized culturing compartments, the HPI device provides a 5-fold reduction of the number of NTS per condition and a 3-fold reduction of compound-solution volumes in comparison to standard visual evaluation methods. Unlike our previously developed platform (Ravaynia et al., 2020), we avoided materials like PDMS that feature unspecific absorption of small molecules and are not suitable for drug screening applications (Figure S10) (van Meer et al., 2017; Torino et al., 2018). In addition, we developed a parallelized, user-friendly, and pump-free system, which was fabricated by using injection molding of polystyrene to reduce costs (~2 CHF per chip) and to increase measurement throughput for large screening applications. By using only standard laboratory plastic materials (PS-PET substrates) for the chips, we could increase the drug assay duration to more than 3 days (Figure S4D), with 72 h being the standard assay time for visual screening. The modular and flexible nature of the HPI device also renders the presented approach widely applicable to other relevant schistosome stages, such as cercariae, juvenile, and small adult parasites (~0.5 mm), or to different parasite species, namely *H. polygyrus*, *A. ceylanicum*, and *N. americanus*, which would help to improve anthelmintic drug screenings.

Moreover, our work demonstrates that impedance-based detection of NTS viability can be applied in medium-to-high throughput assays in accordance with NIH assay guidelines for high-throughput screening applications (Table S1) (Sittampalam et al., 2004). In comparison, a parallelized impedance-based instrument for *in vitro* antischistosomal testing (xWORM), developed by another group, requires a comparably large number of parasites (~500 per well) to assess motility and could not be used to efficiently to monitor schistosomula movements, while larval parasites are the most convenient sample to use for large *in vitro* drug studies (Rinaldi et al., 2015; Tekwu et al., 2016). Alternative detection techniques for parallelized *in vitro* assessment of antischistosomal compounds were also presented in literature. Fluorescence-based and colorimetric-based detection using plate-reader instruments provide a high level of automation. However, to achieve detectable and reliable signals, these methods require 200–400 NTS per well and are limited to end-point analyses that do not provide any information on temporal evolution, which can be captured in impedance-based measurements (Peak et al., 2010; Panic et al., 2015b; Aguiar et al., 2017). Finally, automated image-acquisition systems have been proposed for enabling high-throughput and quantitative analysis of schistosomula phenotypes during drug exposure assays (Lee et al., 2012; Chen et al., 2020). By tracking the temporal evolution of multiple phenotypic aspects, such as parasite morphology, size, and movements, these methods have the potential to produce high-dimensional data with additional information on drug action to support compound optimization, which is most likely missed by monitoring motility alone. For example, a system compatible with high-throughput image acquisition and automated plate handling (SchistoView) was used to evaluate schistosomula at a few discrete time points in a 96-well-plate format and yielded more than 15 parameters for describing parasite phenotypes (Chen et al., 2020). However, SchistoView requires large volume data storage (~15 MB per unit per time point as opposed to ~0.8 MB per unit per time point for impedance) and significant computational resources for analyzing complex phenotypic data. Despite effective strategies for data compression and for reducing the complexity of multiple time-varying parameters, such as the use of time-series analysis and rapid segmentation of NTS in video frames (Lee et al., 2012; Asarnow and Singh, 2013; Singh et al., 2018), image-based approaches require comparably long acquisition time (~1 h per time point for a 96-well plate) and dedicated equipment for well-plate handling when performing large screening assays, which may impact temporal resolution and system scalability in comparison to using impedance-based readouts.

## Conclusion

In conclusion, we developed an automated highly parallel, impedance-based system, which can be used to continuously assess the efficacy of drugs on NTS during more than 72 h *in vitro* testing. The current layout enables to operate up to 16 chips and 128 analysis units in parallel using a single instrument, while the modularity of the design allows for further upscaling. The device performance was demonstrated in single-dose screenings and dose-response analyses and requires minimal operator interference. The system modularity and throughput, the use of standard plastic materials for component fabrication, and in particular, the large amount of information that is available through continuous monitoring of NTS responses to compounds will help to significantly advance preclinical antischistosomal studies. Finally, the identification of hit compounds during the screening reported here demonstrates the potential of our device for discovering new drugs to treat schistosomiasis.

## Limitations of the study

This drug screening study is based on the continuous monitoring of *S. mansoni* larvae responses against a collection of drugs from the MMV Pandemic Response Box using our developed impedance-based platform. From our larval assays, we were able to identify four antischistosomal hit drugs with high *in vitro* potency, fast action, and low cytotoxicity. However, to confirm the suitability of the four drugs for schistosomiasis drug development, future studies should include and demonstrate the efficacy of those compounds against adult-stage schistosomes in *in vitro* and *in vivo* tests. In addition, in contrast to the large-scale production of schistosomula samples, the acquisition of adult schistosomes from infected animals is very laborious and is not suitable for the implementation of medium-throughput or high-throughput approaches for drug screening at present. Therefore, in our antischistosomal study, we discussed exclusively works and systems that have been applied to larval-stage schistosomes.

## STAR★METHODS

Detailed methods are provided in the online version of this paper and include the following:

- KEY RESOURCES TABLE

- RESOURCE AVAILABILITY
  - Lead contact
  - Materials availability
  - Data and code availability
- EXPERIMENTAL MODEL AND SUBJECT DETAILS
  - Parasite preparation
- METHOD DETAILS
  - Compounds and culture media
  - *In vitro* visual drug-sensitivity assay
  - Larval impedance-based drug assay
  - Plastic chip fabrication
  - Chip preparation
  - Platform assembly
  - Impedance-based measurement and setup
  - Absorption evaluation on chip
  - Imaging
- QUANTIFICATION AND STATISTICAL ANALYSIS

## AUTHOR CONTRIBUTIONS

P.S.R. designed and developed the HPI device, planned and performed all experiments, analyzed the data, and wrote the manuscript. S.B. planned and performed all experiments, analyzed the data, and edited the manuscript. F.G. analyzed the data and edited the manuscript. J.K. and A.H. coordinated and conceived the project, were involved in the scientific considerations, and edited the manuscript. M.M.M. conceived the project, interpreted data, and edited the manuscript.

## DECLARATION OF INTERESTS

The authors declare no competing interests.

## REFERENCES

Abdulla, M.-H., Ruelas, D.S., Wolff, B., Snedecor, J., Lim, K.-C., Xu, F., Renslo, A.R., Williams, J., McKerrow, J.H., and Caffrey, C.R. (2009). Drug discovery for schistosomiasis: hit and lead compounds identified in a library of known drugs by medium-throughput phenotypic screening. PLoS Negl. Trop. Dis. *3*, e478. https://doi.org/10.1371/journal.pntd.0000478.

Adenowo, A.F., Oyinloye, B.E., Ogunyinka, B.I., and Kappo, A.P. (2015). Impact of human schistosomiasis in sub-Saharan Africa. Braz. J. Infect. Dis. *19*, 196–205. https://doi.org/10.1016/j.bjid.2014.11.004.

Aguiar, P.H.N., Fernandes, N.M.G.S., Zani, C.L., and Mourão, M.M. (2017). A high-throughput colorimetric assay for detection of Schistosoma mansoni viability based on the tetrazolium salt XTT. Parasit. Vectors *10*, 300–310. https://doi.org/10.1186/s13071-017-2240-3.

Asarnow, D.E., and Singh, R. (2013). Segmenting the etiological agent of schistosomiasis for high-content screening. IEEE Trans. Med. Imaging *32*, 1007–1018. https://doi.org/10.1109/TMI.2013.2247412.

Bergquist, R., Utzinger, J., and Keiser, J. (2017). Controlling schistosomiasis with praziquantel: how much longer without a viable alternative? Infect. Dis. Poverty *6*, 1–10. https://doi.org/10.1186/s40249-017-0286-2.

Biendl, S., Häberli, C., and Keiser, J. (2021). Discovery of novel antischistosomal scaffolds

from the open access Pandemic Response Box. Expert Rev. Anti Infect. Ther. 1–9. https://doi.org/10.1080/14787210.2022.1990042.

Chawla, K., Modena, M.M., Ravaynia, P.S., Lombardo, F.C., Leonhardt, M., Panic, G., Bürgel, S.C., Keiser, J., and Hierlemann, A. (2018). Impedance-based microfluidic assay for automated antischistosomal drug screening. ACS Sens. 3, 2613–2620. https://doi.org/10.1021/acssensors.8b01027.

Chen, S., Suzuki, B.M., Dohrmann, J., Singh, R., Arkin, M.R., and Caffrey, C.R. (2020). A multi-dimensional, time-lapse, high content screening platform applied to schistosomiasis drug discovery. Commun. Biol. 3, 747. https://doi.org/10.1038/s42003-020-01402-5.

Conteh, L., Engels, T., and Molyneux, D.H. (2010). Socioeconomic aspects of neglected tropical diseases. Lancet 375, 239–247. https://doi.org/10.1016/S0140-6736(09)61422-7.

Ferrari, M.L., Coelho, P.M., Antunes, C.M., Tavares, C.A., and da Cunha, A.S. (2003). Efficacy of oxamniquine and praziquantel in the treatment of Schistosoma mansoni infection: a controlled trial. Bull. World Health Organ. 81, 190–196. https://doi.org/10.1590/S0042-96862003000300009.

Ghose, A.K., and Crippen, G.M. (1987). Atomic physicochemical parameters for three-dimensional-structure-directed quantitative structure-activity relationships. 2. Modeling dispersive and hydrophobic interactions. J. Chem. Inf. Comput. Sci. 27, 21–35. https://doi.org/10.1021/ci00053a005.

Gryseels, B. (2012). Schistosomiasis. Infect. Dis. Clin. North Am. 26, 383–397. https://doi.org/10.1016/j.idc.2012.03.004.

Keiser, J. (2010). In vitro and in vivo trematode models for chemotherapeutic studies. Parasitology 137, 589–603. https://doi.org/10.1017/S0031182009991739.

Koehne, E., Zander, N., Rodi, M., Held, J., Hoffmann, W., Zoleko-Manego, R., Ramharter, M., Mombo-Ngoma, G., Kremsner, P.G., and Kreidenweiss, A. (2021). Evidence for in vitro and in vivo activity of the antimalarial pyronaridine against Schistosoma. PLoS Negl. Trop. Dis. 15, e0009511. https://doi.org/10.1371/journal.pntd.0009511.

Kyu, H.H., Abate, D., Abate, K.H., Abay, S.M., Abbafati, C., Abbasi, N., Abbastabar, H., Abd-Allah, F., Abdela, J., Abdelalim, A., et al. (2018). Global, regional, and national disability-adjusted life-years (DALYs) for 359 diseases and injuries and healthy life expectancy (HALE) for 195 countries and territories, 1990–2017: a systematic analysis for the Global Burden of Disease Study 2017. Lancet 392, 1859–1922. https://doi.org/10.1016/S0140-6736(18)32335-3.

Lee, H., Moody-Davis, A., Saha, U., Suzuki, B.M., Asarnow, D., Chen, S., Arkin, M., Caffrey, C.R., and Singh, R. (2012). Quantification and clustering of phenotypic screening data using time-series analysis for chemotherapy of schistosomiasis. BMC Genomics 13, S4. https://doi.org/10.1186/1471-2164-13-S1-S4.

Lipinski, C.A., Lombardo, F., Dominy, B.W., and Feeney, P.J. (2012). Experimental and

computational approaches to estimate solubility and permeability in drug discovery and development settings. Adv. Drug Deliv. Rev. 64, 4–17. https://doi.org/10.1016/j.addr.2012.09.019.

Lohasz, C., Rousset, N., Renggli, K., Hierlemann, A., and Frey, O. (2019). Scalable microfluidic platform for flexible configuration of and experiments with microtissue multiorgan models. SLAS Technol. 24, 79–95. https://doi.org/10.1177/2472630318802582.

Lombardo, F.C., Pasche, V., Panic, G., Endriss, Y., and Keiser, J. (2019). Life cycle maintenance and drug-sensitivity assays for early drug discovery in Schistosoma mansoni. Nat. Protoc. 14, 461–481. https://doi.org/10.1038/s41596-018-0101-y.

Macarrón, R., and Hertzberg, R.P. (2011). Design and implementation of high throughput screening assays. Mol. Biotechnol. 47, 270–285. https://doi.org/10.1007/s12033-010-9335-9.

Maccesi, M., Aguiar, P.H.N., Pasche, V., Padilla, M., Suzuki, B.M., Montefusco, S., Abagyan, R., Keiser, J., Mourão, M.M., and Caffrey, C.R. (2019). Multi-center screening of the Pathogen Box collection for schistosomiasis drug discovery. Parasit. Vectors 12, 493. https://doi.org/10.1186/s13071-019-3747-6.

Marcellino, C., Gut, J., Lim, K.C., Singh, R., McKerrow, J., and Sakanari, J. (2012). WormAssay: a novel computer application for whole-plate motion-based screening of macroscopic parasites. PLoS Negl. Trop. Dis. 6, e1494. https://doi.org/10.1371/journal.pntd.0001494.

McManus, D.P., Dunne, D.W., Sacko, M., Utzinger, J., Vennervald, B.J., and Zhou, X.N. (2018). Schistosomiasis. Nat. Rev. Dis. Primers 4, 13. https://doi.org/10.1038/s41572-018-0013-8.

Milligan, J.N., and Jolly, E.R. (2011). Cercarial transformation and in vitro cultivation of Schistosoma mansoni schistosomules. J. Vis. Exp. 1–4. https://doi.org/10.3791/3191.

Modena, M.M., Chawla, K., Lombardo, F., Bürgel, S.C., Panic, G., Keiser, J., and Hierlemann, A. (2017). Impedance-based detection of Schistosoma mansoni larvae viability for drug screening. IEEE Biomed. Circuits Syst. Conf. 2017, 17693744.

Molehin, A.J. (2020). Schistosomiasis vaccine development: update on human clinical trials. J. Biomed. Sci. 27, 28. https://doi.org/10.1186/s12929-020-0621-y.

Olveda, R.M., Tallo, V., Olveda, D.U., Inobaya, M.T., Chau, T.N., and Ross, A.G. (2016). National survey data for zoonotic schistosomiasis in the Philippines grossly underestimates the true burden of disease within endemic zones: implications for future control. Int. J. Infect. Dis. 45, 13–17. https://doi.org/10.1016/j.ijid.2016.01.011.

Panic, G., Duthaler, U., Speich, B., and Keiser, J. (2014). Repurposing drugs for the treatment and control of helminth infections. Int. J. Parasitol. Drugs Drug Resist. 4, 185–200. https://doi.org/10.1016/j.ijpddr.2014.07.002.

Panic, G., Vargas, M., Scandale, I., and Keiser, J. (2015a). Activity profile of an FDA-approved compound library against schistosoma mansoni.

PLoS Negl. Trop. Dis. 9, e0003962. https://doi.org/10.1371/journal.pntd.0003962.

Panic, G., Flores, D., Ingram-Sieber, K., and Keiser, J. (2015b). Fluorescence/luminescence-based markers for the assessment of Schistosoma mansoni schistosomula drug assays. Parasit. Vectors 8, 624. https://doi.org/10.1186/s13071-015-1233-3.

Paveley, R.A., Mansour, N.R., Hallyburton, I., Bleicher, L.S., Benn, A.E., Mikic, I., Guidi, A., Gilbert, I.H., Hopkins, A.L., and Bickle, Q.D. (2012). Whole organism high-content screening by label-free, image-based Bayesian classification for parasitic diseases. PLoS Negl. Trop. Dis. 6. e1762–11. https://doi.org/10.1371/journal.pntd.0001762.

Peak, E., and Hoffmann, K.F. (2011). Cross-disciplinary approaches for measuring parasitic helminth viability and phenotype. An. Acad. Bras. Cienc. 83, 649–662. https://doi.org/10.1590/s0001-37652011000200024.

Peak, E., Chalmers, I.W., and Hoffmann, K.F. (2010). Development and validation of a quantitative, high-throughput, fluorescent-based bioassay to detect schistosoma viability. PLoS Negl. Trop. Dis. 4, e759. https://doi.org/10.1371/journal.pntd.0000759.

Pedrique, B., Strub-Wourgaft, N., Some, C., Olliaro, P., Trouiller, P., Ford, N., Pécoul, B., and Bradol, J.H. (2013). The drug and vaccine landscape for neglected diseases (2000-11): a systematic assessment. Lancet Glob. Health 1, e371–e379. https://doi.org/10.1016/S2214-109X(13)70078-0.

Ramirez, B., Bickle, Q., Yousif, F., Fakorede, F., Mouries, M.A., and Nwaka, S. (2007). Schistosomes: challenges in compound screening. Expert Opin. Drug Discov. 2, S53–S61. https://doi.org/10.1517/17460441.2.S1.S53.

Ravaynia, P.S., Lombardo, F.C., Biendl, S., Dupuch, M.A., Keiser, J., Hierlemann, A., and Modena, M.M. (2020). Parallelized impedance-based platform for continuous dose-response characterization of antischistosomal drugs. Adv. Biosyst. 4. e1900304–12. https://doi.org/10.1002/adbi.201900304.

Reader, J., van der Watt, M.E., Taylor, D., Le Manach, C., Mittal, N., Ottilie, S., Theron, A., Moyo, P., Erlank, E., Nardini, L., et al. (2021). Multistage and transmission-blocking targeted antimalarials discovered from the open-source MMV Pandemic Response Box. Nat. Commun. 12, 269. https://doi.org/10.1038/s41467-020-20629-8.

Rinaldi, G., Loukas, A., Brindley, P.J., Irelan, J.T., and Smout, M.J. (2015). Viability of developmental stages of Schistosoma mansoni quantified with xCELLigence worm real-time motility assay (xWORM). Int. J. Parasitol. Drugs Drug Resist. 5, 141–148. https://doi.org/10.1016/j.ijpddr.2015.07.002.

Sasaki, H., Onoe, H., Osaki, T., Kawano, R., and Takeuchi, S. (2010). Parylene-coating in PDMS microfluidic channels prevents the absorption of fluorescent dyes. Sensors Actuators B Chem. 150, 478–482. https://doi.org/10.1016/j.snb.2010.07.021.

Silva-Moraes, V., Couto, F.F., Vasconcelos, M.M., Araújo, N., Coelho, P.M., Katz, N., and Grenfell, R.F. (2013). Antischistosomal activity of a calcium channel antagonist on schistosomula and adult Schistosoma mansoni worms. Mem. Inst. Oswaldo Cruz *108*, 600–604. https://doi.org/10.1590/0074-0276108052013011.

Singh, R., Pittas, M., Heskia, I., Xu, F., McKerrow, J., and Caffrey, C.R. (2009). Automated image-based phenotypic screening for high-throughput drug discovery. In 2009 22nd IEEE International Symposium on Computer-based Medical Systems (IEEE), pp. 1–8. https://doi.org/10.1109/CBMS.2009.5255338.

Singh, R., Beasley, R., Long, T., and Caffrey, C.R. (2018). Algorithmic mapping and characterization of the drug-induced phenotypic-response space of parasites causing schistosomiasis. IEEE/ACM Trans. Comput. Biol. Bioinform. *15*, 469–481. https://doi.org/10.1109/TCBB.2016.2550444.

G.S. Sittampalam, A. Grossman, K. Brimacombe, M. Arkin, D. Auld, C.P. Austin, J. Baell, T.D.Y. Chung, N.P. Coussens, and J.L. Dahlin, et al., eds. (2004). Assay Guidance Manual (Eli Lilly & Company and the National Center for Advancing Translational Sciences). https://www.ncbi.nlm.nih.gov/books/NBK53196/.

Sun, T., and Morgan, H. (2010). Single-cell microfluidic impedance cytometry: a review. Microfluid. Nanofluid. *8*, 423–443. https://doi.org/10.1007/s10404-010-0580-9.

Tekwu, E.M., Anyan, W.K., Boamah, D., Baffour-Awuah, K.O., Keyetat Tekwu, S., Penlap Beng, V., Nyarko, A.K., and Bosompem, K.M. (2016). Mechanically produced schistosomula as a higher-throughput tools for phenotypic pre-screening in drug sensitivity assays: current research and future trends. Biomark. Res. *4*, 21. https://doi.org/10.1186/s40364-016-0075-2.

Toepke, M.W., and Beebe, D.J. (2006). PDMS absorption of small molecules and consequences in microfluidic applications. Lab Chip *6*, 1484–1486. https://doi.org/10.1039/b612140c.

Torino, S., Corrado, B., Iodice, M., and Coppola, G. (2018). Pdms-based microfluidic devices for cell culture. Inventions *3*, 1–14. https://doi.org/10.3390/inventions3030065.

Trouiller, P., Olliaro, P., Torreele, E., Orbinski, J., Laing, R., and Ford, N. (2002). Drug development for neglected diseases: a deficient market and a public-health policy failure. Lancet *359*, 2188–2194. https://doi.org/10.1016/S0140-6736(02)09096-7.

van Meer, B.J., de Vries, H., Firth, K.S.A., van Weerd, J., Tertoolen, L.G.J., Karperien, H.B.J., Jonkheijm, P., Denning, C., IJzerman, A.P., and Mummery, C.L. (2017). Small molecule absorption by PDMS in the context of drug response bioassays. Biochem. Biophys. Res. Commun. *482*, 323–328. https://doi.org/10.1016/j.bbrc.2016.11.062.

Van Midwoud, P.M., Janse, A., Merema, M.T., Groothuis, G.M., and Verpoorte, E. (2012). Comparison of biocompatibility and adsorption properties of different plastics for advanced microfluidic cell and tissue culture models. Anal. Chem. *84*, 3938–3944. https://doi.org/10.1021/ac300771z.

Vale, N., Gouveia, M.J., Rinaldi, G., Brindley, P.J., Gärtner, F., and Correia da Costa, J.M. (2017). Praziquantel for schistosomiasis: single-drug metabolism revisited, mode of action, and resistance. Antimicrob. Agents Chemother. *61*, 1–16. https://doi.org/10.1128/AAC.02582-16.

Vos, T., Abajobir, A.A., Abate, K.H., Abbafati, C., Abbas, K.M., Abd-Allah, F., Abdulkader, R.S., Abdulle, A.M., Abebo, T.A., Abera, S.F., et al. (2017). Global, regional, and national incidence, prevalence, and years lived with disability for 328 diseases and injuries for 195 countries, 1990-2016: a systematic analysis for the Global Burden of Disease Study 2016. Lancet *390*, 1211–1259. https://doi.org/10.1016/S0140-6736(17)32154-2.

Wang, W., Wang, L., and Liang, Y.S. (2012). Susceptibility or resistance of praziquantel in human schistosomiasis: a review. Parasitol. Res. *111*, 1871–1877. https://doi.org/10.1007/s00436-012-3151-z.

Weng, H.B., Chen, H.X., and Wang, M.W. (2018). Innovation in neglected tropical disease drug discovery and development. Infect. Dis. Poverty *7*, 67. https://doi.org/10.1186/s40249-018-0444-1.

## STAR★METHODS

### KEY RESOURCES TABLE

| REAGENT or RESOURCE | SOURCE | IDENTIFIER |
|---|---|---|
| **Chemicals, peptides, and recombinant proteins** | | |
| Pandemic Response Box | Medicines for Malaria Venture | https://www.mmv.org/mmv-open/pandemic-response-box |
| Methylene blue | Sigma-Aldrich | M9140-25G |
| Mefloquine | Sigma-Aldrich | M2319-100MG |
| Praziquantel | Sigma-Aldrich | P4668-5G |
| Dimethyl sulfoxide | Sigma-Aldrich | D2650-5X5ML |
| Rhodamine-B | Sigma-Aldrich | 83689 |
| Biolipidure | NOF America Corporation | 206 |
| Medium 199 | Gibco | 22340-020 |
| Inactivated fetal calf serum | Bioconcept AG | 2-01F30-I |
| Penicillin and streptomycin | Bioconcept AG | P4333-100ML |
| **Experimental models: Organisms/strains** | | |
| *S. mansoni* newly transformed schistosomula | Laboratory of Prof. Jennifer Keiser, TPH | https://www.niaid.nih.gov/research/schistosomiasis-resource-center |
| **Software and algorithms** | | |
| Matlab | The MathWorks Inc. | R2018b |
| Python | Python Software Foundation License | 3.5.2 |
| RDKit | Open-Source Cheminformatics | 2020.09.2 |
| **Other** | | |
| Double-sided adhesive tape | 3M Company | 468MP |
| Polyethylene terephthalate foil | Goodfellow Cambridge Ltd | ES301400 |
| Injection-molded polystyrene | Protolabs | https://www.protolabs.co.uk/services/injection-moulding/plastic-injection-moulding/ |
| Impedance spectroscope | Zurich Instruments AG | HF2-LI |
| Optical microscope | Nikon | Ti-E |
| Microplate reader | Tecan | Infinite M200 Pro |

## RESOURCE AVAILABILITY

### Lead contact

Further information and other requests should be directed to and will be fulfilled by the lead contact, Paolo S. Ravaynia (paolo.ravaynia@bsse.ethz.ch).

### Materials availability

This study did not generate new unique reagents.

### Data and code availability

- All data produced in this study are included in the published article and its supplemental information, or are available from the Lead contact upon request.

- This paper does not report original code.

- Any additional information required to reanalyze the data reported in this paper is available from the Lead contact upon request.

## EXPERIMENTAL MODEL AND SUBJECT DETAILS

### Parasite preparation

Cercariae of *S. mansoni* were obtained from infected intermediate host snails (*Biomphalaria glabrata*) and mechanically transformed to newly transformed schistosomula (NTS) as described previously (Milligan and Jolly, 2011; Lombardo et al., 2019). In brief, *S. mansoni*-infected *B. glabrata* snails were placed singularly in 24-well plates and exposed to a neon lamp (36 W, 4000 K, 3350 lumens) for 3-4 h to induce the shedding of cercariae. The supernatant was collected and filtered to remove impurities in the suspension. The mechanical transformation of the cercariae into NTS was performed by physically removing the tail by constricted passage through a Luer-Lok tip in between two 12 mL syringes. After washing in Hanks' balanced salt solution (HBSS, cat. no. 14175, Gibco, Waltham, USA), supplemented with 1% penicillin (10000 U/ml) and streptomycin (10 mg/ml) solution, NTS were re-suspended in M199 culture medium and kept overnight at 37°C and 5% $CO_2$.

## METHOD DETAILS

### Compounds and culture media

The 400 compounds contained in the drug library, termed "Pandemic Response Box" (PRB), were provided by Medicines for Malaria Venture (MMV, Geneva, Switzerland) in five 96-well plates, dissolved in 10 µL of pure dimethyl sulfoxide (DMSO) at a concentration of 10 mM. These stock solutions were further diluted (1:10) in DMSO (cat. no. D2650-5X5ML, Sigma-Aldrich, Buchs, Switzerland), aliquoted and stored at -20°C until further use. Reference compounds, methylene blue (cat. no. M9140-25G, Sigma-Aldrich, Buchs, Switzerland), mefloquine (cat. no. M2319-100MG, Sigma-Aldrich, Buchs, Switzerland), and praziquantel (cat. no. P4668-5G, Sigma-Aldrich, Buchs, Switzerland) were purchased as racemic powders, and solutions were freshly prepared on the day of the experiment with a concentration of 10 mM in DMSO (Silva-Moraes et al., 2013; Ravaynia et al., 2020; Koehne et al., 2021).

M199 culture medium, which was used for incubation and *in vitro* drug assays of *S. mansoni* newly transformed schistosomula (NTS), was prepared by supplementing Medium 199 (cat. no. 22340-020, Gibco, Waltham, USA) with 1% penicillin (10000 U/ml) and streptomycin (10 mg/ml) solution (pen/strep, cat. no. P4333-100ML, Bioconcept AG, Allschwil, Switzerland) and 5% v/v inactivated fetal calf serum (iFCS, cat. no. 2-01F30-I, Bioconcept AG, Allschwil, Switzerland).

All media were sterilized by filtration using a 0.22-µm-filter bottle (cat. no. 431097-COR, Vitaris AG, Baar, Switzerland).

### *In vitro* visual drug-sensitivity assay

The 400 compounds contained in the PRB compound library were initially screened for their activity against NTS following the standard screening procedure based on visual scoring (Lombardo et al., 2019). In brief, approximately 50-100 NTS were incubated in culture medium with the test compounds at 10 µM (in a final volume of 200 µL) at 37°C, 5% $CO_2$ for 3 days in 96-well plates (cat. no. 83.3924, Sarstedt, Nümbrecht, Germany). After 72 h of incubation, a trained operator evaluated the NTS phenotype by microscopic readout (magnification 10-40×, Carl Zeiss, Jena, Germany) using a viability scale from 0 (dead) to 3 (healthy and motile parasites) estimating death, changes in motility, and morphological alterations.

For all experiments, the highest concentration of DMSO (0.5% v/v) in culture medium served as control. For *in vitro* phenotypic drug sensitivity assays, each experimental condition was tested in triplicates and repeated at least once.

### Larval impedance-based drug assay

The drug assay in the plastic chips was carried out in three main steps: (i) medium pre-wetting procedure at day -1, (ii) parasite loading at day 0 and (iii) drug addition after 1 h of NTS culturing in the microwells. On the day before the assay, the pre-wetting procedure was performed by dispensing 30 µL of plain M199 medium in all 128 microwells. The assembled platforms were subsequently inserted in a vacuum desiccator (Nalgene 5310-0250, Sigma-Aldrich, Buchs, Switzerland) for 10 min to degas the medium. After the degassing

step, the chips were kept in the incubator at 37°C and 5% $CO_2$ overnight. On the day of the assay, the plain pre-wetting medium was used to record 30-min signal traces to establish the baseline noise background in each microwell before the insertion of the larvae. After that, 25 μL of pre-wetting medium were removed from each microwell, and 30 μL of larvae solution with 0.7 NTS μL$^{-1}$ were dispensed to each unit. The signal fluctuations caused by untreated NTS were acquired for 1 h to establish baseline parasite activity and for calculating the respective motility index of each microwell. Finally, 30 μL of drug solution were loaded in each microwell, resulting a final volume of 65 μL per analysis unit.

In the drug-screening phase, all compounds were tested at a fixed concentration of 10 μM, whereas in the dose-response assay the overall drug concentrations ranged between 1.5 and 50 μM (1.5, 3, 6, 12, 25 and 50 μM). In each drug experiment, 0.5% v/v DMSO (vehicle control) and plain M199 medium controls were included, and all conditions were evaluated in quadruplicates. For the drug-screening assay, two HPI systems (four stacked platforms per system) were used, whereas for the dose-response characterization we adopted a single HPI system (including four platforms). Only new, unused chips were employed for each experiment. Impedance-based larval motility and viability indices for each test condition were measured every 16 min during 72 h in each platform. The viability index ranged from 0 to 1 (0 = no fluctuations, dead parasites; 1= motile and alive parasites) and was computed by normalizing the NTS motility under each drug exposure with respect to motility in the vehicle control (see Quantification and statistical analysis section for more information).

### Plastic chip fabrication

The 8-microwell chip design was developed based on a previously used poly(dimethylsiloxane) (PDMS) device (Ravaynia et al., 2020). The chip was realized entirely in standard laboratory plastic materials to avoid drug ad/absorption by PDMS during long-term compound testing (Van Midwoud et al., 2012; van Meer et al., 2017). The plastic device consisted of two main parts: a top polystyrene (PS) layer containing 8 microwells and a bottom poly(ethylene terephthalate) (PET) foil, patterned with 8 pairs of co-planar platinum electrodes. The PS layer was fabricated using injection molding, the optimized mold scheme is shown in Figure S1A, all chips were provided by Protolabs (Protolabs, Feldkirchen, Germany) at costs of ∼2 CHF per unit. The injection and ejection mark points of the PS parts were chosen so as to not interfere with the bonding of the bottom to the PET slide (Figure S1B). The 200-nm-thick platinum electrodes were deposited on a 6-inch laser-cut PET wafer (ES301400 PET Film, Goodfellow Cambridge Ltd, Huntingdon, England) via a shadow-mask process. Briefly, a metal mask (1.4310 +C1300 20mm, Lasercut AG, Bäretswil, Switzerland) was mounted on the PET wafer with a magnetic holder located underneath. After 40 min of platinum sputtering, the PET wafer was diced into 10 individual slides by laser-cutting (Figures S1C and S1D). Finally, each PS chip and patterned PET slide were aligned using a custom-made alignment tool and bonded with double-sided adhesive tape (468MP, 3M Company, Saint Paul, USA).

### Chip preparation

Before the sealing procedure, both PS and PET substrates were cleaned two times by immersion and ultrasonication in isopropanol and dried using an air gun. The PS chips and PET slides were then rendered hydrophilic to facilitate liquid loading during the drug assay by oxygen plasma surface treatment for 40 sec (Harrick Plasma PDC-002, Harrick Plasma, Ithaca, USA) (Van Midwoud et al., 2012). After PS-PET bonding, each microwell was coated with 10 μL of Biolipidure (NOF America Corporation, WhitePlains, NY, USA) and incubated at room temperature for 5 min. Biolipidure solution was withdrawn completely from the microwells using a vacuum pump, and the devices underwent a second coating step to increase long-term surface hydrophilicity. After incubating for another 5 min with Biolipidure, the coating solution was removed again, and all chips were dried overnight and UV-sterilized in a laminar-flow hood.

### Platform assembly

Up to four PS chips were assembled into a platform. Every chip was covered with a laser-cut PS lid to avoid medium evaporation and was placed between a custom-made printed circuit board (PCB) and an aluminum (Al) holder plate (Figure S2A). The PCB design was described in detail elsewhere (Ravaynia et al., 2020). Briefly, the board featured 2 analog SMA connectors as input/output ports for the impedance spectroscope and 64 spring-contact connectors for interfacing with the electrode pads of the four chips. The Al holder was realized by water-jet cutting (EN AW-5083/ 3.3547/ Al-Mg4.5Mn, Xometry Europe GmbH, Ottobrunn, Germany). The holder frame featured four openings to enable microscopy inspection of the parasites in each chip and eight screw holes for adjusting the contact force.

Up to four assembled platforms were then stacked and operated in a single incubator compartment (Figure S2B), allowing for operating 128 microwell units in parallel under identical testing conditions. During 3-day drug assays, the platforms were kept in the incubator at 37°C and 5% $CO_2$.

### Impedance-based measurement and setup

The impedance measurements were performed using a HF2-LI impedance spectroscope (Zurich Instruments AG, Zurich, Switzerland). A 500-kHz voltage signal with an amplitude of 100 mV was applied to the electrode pairs of each microwell unit. The frequency of the sinusoidal carrier signal (500 kHz) was chosen to enable fast multiplexing (1.5 μs) between all the units and to minimize the signal attenuation in the platforms ($\sim-29$ dBV in magnitude, Figure S3). The AC current was then converted to a voltage signal through a trans-impedance amplifier (HF2TA, Zurich Instruments AG, Zurich, Switzerland) with a 1-kΩ feedback resistor, digitalized at a sampling frequency of 14 kHz and filtered with a 2.2-kHz low pass. A custom-made Python software, installed on a control PC station, was implemented to define the selection scheme of the microwells over the four parallel platforms and the switching-time protocol of the signal recordings. In each platform, the signal of each electrode pair was recorded for 1 ms before switching to the following unit. This procedure enabled continuous and quasi-parallel acquisition from all wells within a platform at a sampling frequency of $\sim$32 Hz. The AC signal from all wells in a platform was acquired for 1 minute and every 16 minutes throughout the assay. The voltage signal magnitude was then used for further analysis (see section Quantification and statistical analysis for more information).

### Absorption evaluation on chip

PS is a validated material for cell-culture applications and offers substantial advantages over PDMS for use with microfluidic systems for *in vitro* drug testing (Toepke and Beebe, 2006; Sasaki et al., 2010; Van Midwoud et al., 2012; Lohasz et al., 2019; Ravaynia et al., 2020). To confirm that PS did not feature substantial molecule absorption, 50 μL of 100 μM rhodamine-B (83689, Sigma-Aldrich, Buchs, Switzerland) solution were loaded into the microwells and incubated for 24 hours (Lohasz et al., 2019). Fluorescence images of the microwells were captured before the loading of the dye, at 1 and 24 h after sample loading, and after wash-out of the dye by means of an inverted microscope (Nikon Ti-E, Nikon, Egg, Switzerland), as shown in Figure S10A. The single chip was incubated at 37°C and 5% $CO_2$. After 1 day of dye incubation, 50 μL of supernatant solution of each microwell unit were collected and compared to 50 μL of rhodamine B reference solutions (1.5, 3.3, 6.2, 12.5, 25, 50, and 100 μM), which were incubated in a 96-well microplate (675090, Greiner Bio-One GmbH, St. Gallen, Switzerland). The relative fluorescence intensity of all samples was measured using a microplate reader (Infinite M200 Pro, TECAN, Männedorf, Switzerland) at 550 nm excitation - 580 nm emission (Figure S10B). All conditions were analyzed in quadruplicates.

### Imaging

For additional NTS phenotypic evaluation, bright-field images of the parasites, incubated with the PRB compounds in the microwells, were acquired after 72 h using an inverted microscope (Nikon Ti-E, Nikon, Egg, Switzerland) with a Nikon Plan Fluor 10X objective (NA 0.3, WD 16 mm).

## QUANTIFICATION AND STATISTICAL ANALYSIS

The data analysis was performed using custom scripts in MATLAB R2018b (The MathWorks Inc., Natick, USA). The recorded signal magnitude was filtered using a high-pass filter at 0.2 Hz to remove slow baseline drift due to medium evaporation during multi-day assays. To reduce baseline differences between microwell measurements, related to diverse drug solution compositions or drug concentrations, the high-pass-filtered signals were normalized with respect to the mean baseline signal of the respective microwell compartment. To quantify the signal fluctuations induced by NTS movements, the power of the filtered and normalized signal was computed in a 1-3 Hz bandwidth. Only the signals exhibiting an average power above -20 dBμ, which corresponded to a signal-to-noise ratio of > 10, in the first hour of measurements before drug loading were considered for analysis. To compare measurements with different numbers of larvae across the 128 microwells and to extract the motility index parameter, the power of the signal fluctuations arising from treated NTS ($Power_{treated}$) in each unit (i) was normalized with respect to fluctuation power, which was calculated from the measurements of the untreated NTS during the first hour after loading and prior to drug exposure ($Power_{untreated}$ ($t_{-1h}$)). To remove the effect of noise of the readout electronics in the system, the noise power ($Power_{noise}$) was acquired 30 min before the loading of the larvae and was subtracted from all computed signal powers. Thus, the motility index was defined as

$$\text{Motility index}\,(i, t) = \frac{\text{Power}_{treated}\,(i, t) - \text{Power}_{noise}(i)}{\text{Power}_{untreated}(i, t_{-1h}) - \text{Power}_{noise}\,(i)}$$

Subsequently, the NTS viability ratio was calculated by normalizing the motility index of every condition with respect to the motility index of the vehicle control (DMSO). Every condition was analyzed in quadruplicates.

The half-maximum inhibitory concentration ($IC_{50}$) values of the selected drugs were calculated from the impedance-based viability estimations by applying a nonlinear least-squares analysis. A two-parameter sigmoid function with a constant hill slope was fitted to the viability data of each hit. An average hill slope, computed across 72 h of continuous impedance-based characterization of each compound, was applied to the fit for assessment of the $IC_{50}$ values over time. In the dose-response analysis, a maximum viability value of 1 was assigned to all units in which the NTS exhibited a motility equal to or higher than that of the vehicle control (DMSO).

The visual viability scores of the compounds of the PRB library were obtained by averaging across triplicates and normalizing to the vehicle-control (DMSO) viability.

Z'-factor and signal window scores, which provide information on the suitability of a system for high-throughput screening applications, were computed following the NIH assay guidance manual (Sittampalam et al., 2004). Two types of motility indices and their respective variations were analyzed to assess system suitability to detect active compounds during a screen: (i) positive-control motility representing the maximum output obtained with parasites exposed to only the drug vehicle (DMSO) and (ii) negative-control motility originating from the noise background upon M199 medium incubation of the chip. In our experiments, only the assays showing Z-factor scores higher than 0.5 and signal windows above 2 were considered for drug efficacy evaluation (Z-factor: $0.61 \pm 0.05$, Signal-window: $5.50 \pm 1.54$, Table S1).

Physicochemical properties of the hit compounds were calculated using the RDKit (version 2020.09.2) from Open-Source Cheminformatics (available online, https://www.rdkit.org/). The *in silico* analysis was performed to assess conformity with Lipinski's rules considering the molecular weight, the lipophilicity (AlogP, atom-based method by Ghose and Crippen), the number of H-bond acceptors and the number of H-bond donors (Ghose and Crippen, 1987; Lipinski et al., 2012).

All results are displayed as mean values with error bars representing the standard error of the mean (SE), unless specified otherwise. To compare samples from more than two populations, the Kruskal-Wallis H test was adopted. In case the null hypothesis of the test that the distribution of the dependent variables is the same in the studied populations was rejected, a post-hoc Dunn test with Sidák correction was performed for multiple comparisons (Dunn-Sidák multiple-comparison test). Sample sizes and data presentation are specified in each figure caption.